TECHNISCHE
UNIVERSITÄT
WIEN
Vienna University of Technology

UNIVERSITY OF
BELGRADE
Faculty of Mechanical
Engineering

XXIII INTERNATIONAL CONFERENCE ON "MATERIAL HANDLING, CONSTRUCTIONS AND LOGISTICS"

18th – 20th September, 2019

MHCL 2019

Edited by

Georg Kartnig, Nenad Zrnić and Srđan Bošnjak

VIENNA UNIVERSITY OF TECHNOLOGY (TU WIEN)
Institute for Engineering Design and Product Development

together with

UNIVERSITY OF BELGRADE
Faculty of Mechanical Engineering

VIENNA, AUSTRIA, 2019

INTERNATIONAL SCIENTIFIC COMMITTEE

Co-Chairmen:

Prof. Dr. Georg Kartnig, Vienna University of Technology, Austria
Prof. Dr. Nenad Zrnić, University of Belgrade, Serbia
Prof. Dr. Srđan Bošnjak, University of Belgrade, Serbia

Members of Scientific Committee:

Prof. Dr. Bogdevicius Marijonas, Vilnius Gediminas Technical University, Lithuania
Prof. Dr. Bojić Sanja, University of Novi Sad, Serbia
Prof. Dr. Bošnjak Srđan, University of Belgrade, Serbia
Prof. Dr. Ceccarelli Marco, University of Cassino, Italy
Prof. Dr. Chondros Thomas, University of Patras, Greece
Prof. Dr. Clausen Uwe, TU Dortmund, Fraunhofer Institute for Material Flow and Logistic, Germany
Prof. Dr. Ćuprić Nenad, University of Belgrade, Serbia
Prof. Dr. Czmochowski Jerzy, Wroclaw University of Science and Technology, Poland
Prof. Dr. Dentsoras Argiris, University of Patras, Greece
Prof. Dr. Dragović Branislav, University of Montenegro, Kotor, Montenegro
Prof. Dr. Dukić Goran, University of Zagreb, Zagreb, Croatia
Prof. Dr. Edl Milan, University of West Bohemia, Plzen, Czech Republic
Prof. Dr. Ekren Banu, Yaşar University, Turkey
Prof. Dr. Fottner Johannes, Technische Universität München, Germany
Prof. Dr. Furmans Kai, Karsruhe Institute of Technology, Germany
Prof. Dr. Gašić Milomir, University of Kragujevac, Kraljevo, Serbia
Prof. Dr. Gašić Vlada, University of Belgrade, Serbia
Prof. Dr. Georgiev Martin, Technical University Sofia, Bulgaria
Prof. Dr. Georgijević Milosav, University of Novi Sad, Serbia
Prof. Dr. Gerhard Detlef, Vienna University of Technology, Austria
Prof. Dr. Golder Markus, Technischen Universität Chemnitz, Germany
Prof. Dr. Guenthner Wilibald, TU Munich, Germany
Prof. Dr. Illes Bela, University of Miskolc, Hungary
Prof. Dr. Jančevski Janko, Ss. Cyril and Methodius University Skopje, Republic of Macedonia
Prof. Dr. Jerman Boris, University of Ljubljana, Slovenia
Prof. Dr. Jovanović Miomir, University of Niš, Serbia
Prof. Dr. Kartnig Georg, Vienna University of Technology, Austria
Prof. Dr. Katterfeld Andre, Otto-von-Guericke-Universitat Magdeburg, Germany
Prof. Dr. Kessler Franz, Montan University of Leoben, Austria
Prof. Dr. Kosanić Nenad, University of Belgrade, Serbia
Prof. Dr. Kreutzfeldt Jochen, Technische Universität Hamburg, Germany
Prof. Dr. Lerher Tone, University of Maribor, Slovenia
Prof. Dr. Markusik Sylwester, Silesian University of Technology, Gliwice, Poland
Prof. Dr. Mitrović Radivoje, University of Belgrade, Serbia
Prof. Dr. Ognjanović Milosav, University of Belgrade, Serbia
Prof. Dr. Oguamanam C.D. Donatus, Ryerson University Toronto, Ontario, Canada
Prof. Dr. Overmeyer Ludger, Leibniz University Hannover, Germany
Prof. Dr. Park Nam Kyu, Tongmyong Univ. of Information Technology, Busan, South Korea
Prof. Dr. Popović Vladimir, University of Belgrade, Serbia
Prof. Dr. Potrč Iztok, University of Maribor, Slovenia
Prof. Dr. Rakin Marko, University of Belgrade, Serbia
Prof. Dr. Rosi Bojan, University of Maribor, Slovenia
Prof. Dr. Rogić Miroslav, University of Banja Luka, Republic of Srpska, Bosnia and Herzegovina
Prof. Dr. Rusinski Eugeniusz, Wroclaw University of Science and Technology, Poland
Prof. Dr. Sari Zaki, University of Tlemcen, Algeria
Prof. Dr. Savković Mile, University of Kragujevac, Serbia
Prof. Dr. Sawodny Oliver, University of Stuttgart, Germany
Prof. Dr. Schmidt Thorsten, Dresden University of Technology, Germany
Prof. Dr. Schott Dingena, Delft University of Technology, The Netherlands
Prof. Dr. Sihn Wilfried, Vienna University of Technology, Fraunhofer Austria, Austria
Prof. Dr. Singhose William, Georgia Institute of Technology, Atlanta, USA
Prof. Dr. Solazzi Luigi, University of Brescia, Italy
Prof. Dr. ten Hompel Michael, TU Dortmund, Fraunhofer Institute for Material Flow and Logistic, Germany

Prof. Dr. Vidović Milorad, University of Belgrade, Serbia
Prof. Dr. Wehking Karl-Heinz, University of Stuttgart, Germany
Prof. Dr. Weigand Michael, Vienna University of Technology, Austria
Prof. Dr. Wimmer Wolfgang, Vienna University of Technology, Austria
Prof. Dr. Wypych Peter, University of Wollongong, Australia
Prof. Dr. Zrnić Nenad, University of Belgrade, Serbia

President of Honorary Scientific Committee and Conference Founder:

Prof. Dr. Đorđe Zrnić, University of Belgrade, Serbia

Members of Honorary Scientific Committee:

Prof. Dr. Babin Nikola, University of Novi Sad, Serbia
Prof. Dr. Hoffmann Klaus, Vienna University of Technology, Austria
Prof. Dr. Mijajlović Radić, University of Niš, Serbia
Prof. Dr. Oser Joerg, Graz University of Technology, Austria
Prof. Dr. Ostrić Davor, University of Belgrade, Serbia
Prof. Dr. Petković Zoran, University of Belgrade, Serbia
Prof. Dr. Severin Dietrich, Technical University of Berlin, Germany
Prof. Dr. Zrnić Đorđe, University of Belgrade, Serbia

ORGANIZING COMMITEE

Presidents of the Organizing Committee:

Prof. Dr. Georg Kartnig, Vienna University of Technology, Austria
Prof. Dr. Nenad Zrnić, University of Belgrade, Serbia

Vice President of the Organizing Committee:

Prof. Dr. Branislav Dragović, University of Montenegro, Montenegro

Members of Organizing Committee:

Prof. Dr. Gašić Vlada, University of Belgrade, Serbia
Assoc. Prof. Dr. Gnjatović Nebojša, University of Belgrade, Serbia
Alice Grano, Vienna University of Technology, Austria
Milojević Goran, University of Belgrade, Serbia
Đorđević Miloš, University of Belgrade, Serbia
Milenović Ivan, University of Belgrade, Serbia
Stefanović Aleksandar, University of Belgrade, Serbia
Urošević Marko, University of Belgrade, Serbia
Arsić Aleksandra, University of Belgrade, Serbia
Stanković Vlada, University of Belgrade, Serbia

Reviewers:

Prof. Dr. Bošnjak Srđan, Serbia
Prof. Dr. Dragović Branislav, Montenegro
Prof. Dr. Jerman Boris, Slovenia
Prof. Dr. Kartnig Georg, Austria
Prof. Dr. Lerher Tone, Slovenia
Prof. Dr. Zrnić Nenad, Serbia

Publisher:

University of Belgrade, Faculty of Mechanical Engineering

CIRCULATION: 100 copies

ISBN 978-86-6060-020-4

The lateral movement of steel processing belts – extended consideration on belts with low belt tension

Franz Paulischin
Teaching Assistant
Vienna Univercity of Technology
Faculty of Mechanical and Industrial Engineering
Institute for Engineering Design and Product Development

Georg Kartnig
Professor
Vienna Univercity of Technology
Faculty of Mechanical and Industrial Engineering
Institute for Engineering Design and Product Development

Due to the system behaviour, the tracking of steel processing belts is typically performed by the feedback controlled pulley adjustment. There is an analytical model available to describe the lateral running behaviour of the belt, but it was developed for highly tensioned belts. As the belt tension decreases, the model becomes invalid and ultimately unusable. After a presentation of this model the calculated lateral moving behaviour is compared with the results of measurements on a test rig for steel processing belts. In this way, the limits of use for the analytical model with respect to belt tension are shown. Finally, it is demonstrated how the lateral running of a belt can be simulated, especeally by means of the discrete element method.

Keywords: *steel processing belt, belt conveyor, belt misalignment, tracking, DEM*

1. INTRODUCTION

Steel processing belts are special conveyor belts which use a steel belt with a thickness of one to a few millimetres. These conveyors are required, for example, in the chemical industry or in the production of bakery products. Due to the high stiffness of the steel belt, many track guidance systems known from rubber belts cannot be used here. Consequently, steel belts are guided on cylindrical, position-controlled pulleys. The controller is based on a belt model that currently only works satisfactorily for highly-tensioned belts. However, the following applications require low-tensioned belts. Therefore, suitable models are being searched for these low tensioned belts.

- during the start-up-phase of the system starting with the totally untensioned belt e.g. during belt production or the first installation of a belt machine
- in the operation of refurbished plants, when a new belt with larger dimensions (width b, thickness h) runs on existing pulley stations. The maximum permissible belt tensile force is limited by the existing design. The system must be operated with reduced belt tension.

This paper starts with the modelling of the steel belt. After a presentation of existing models for high tensioned belts, the geometric situation at the point of contact is examined more closely. Based on this, ideas for a new approach for low tensioned belts are presented. Finally, this article deals with simulations of the lateral movement of the belt. After a short presentation of an existing FEM model, a new approach in DEM is presented.

Correspondence to: Dipl. Ing. Franz Paulischin, Teaching Assistant, Technische Universität Wien,
Getreidemarkt 9/307-1, 1060 Vienna, Austria
E-mail: franz.paulischin@tuwien.ac.at

2. PULLEY ADJUSTMENT VIA YAW ANGEL β

The regulation of the belt position in y-direction is typically achieved by the inclined position of the tail pulley TP. The yaw angle occurring in this case ranges from a few hundredths to tenths of a degree. In order to be able to clearly illustrate this angle and the resulting effects, the following sketches are shown strongly larger in relation to the yaw angle. The two ends of the axis of the tail pulley TP (Figure 1) are moved in x-direction in the opposite direction by the distance Δx. As a result, the tail pulleys axis yaws by the angle β.

$$\beta = \tan^{-1}\frac{2 * \Delta x}{d} \approx \frac{2 * \Delta x}{d} \tag{1}$$

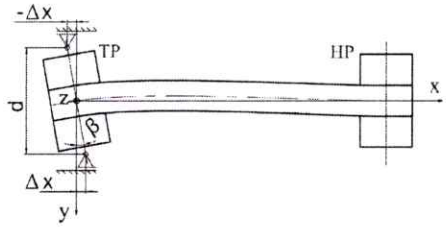

Figure 1. Pulley adjustment in vertical axis

Figure 2 shows a characteristic belt moving curve for the upper span (Figure 3) of a highly tensioned belt. The duration of the transient phase and the amplitudes occurring depend on the belt dimensions and the belt tension.

The following characteristic values can be obtained from the steady-state range:

- steady-state velocity: slope of the curves in the steady-state situation:

$$\dot{y}_1 = \dot{y}_4 = \frac{\Delta y_1}{\Delta x_1} = \frac{\Delta y_4}{\Delta x_4} \tag{2}$$

- steady-state offset: distance in y-direction between the run-up point and the run-off point of a belt span

$$\Delta y_{1-4} = |y_1 - y_4| \quad (3)$$

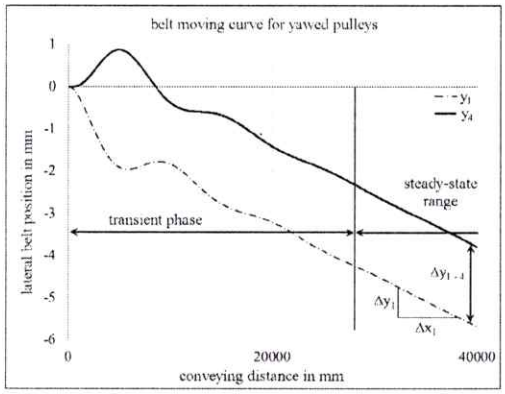

Figure 2. Characteristic belt moving curve

3. MODELLING

In this chapter, the geometric conditions at the point of contact of a flexible rope and a belt on a cylindrical pulley, which is yawed by β, are examined in detail. Thus the lateral moving behaviour of the run-up point of a rope or a belt at a pulley can be determined. Next, a closed rope on a belt conveyor with two cylindrical pulleys is considered. With the help of the rope model - a limp, highly tensioned rope on two pulleys - the movements at the run-up and run-down points (Figure 3, points 1, 3 and 2, 4) as well as the interaction between these points are described. Finally, the beam model [1] [2], a mathematical model for highly tensioned steel processing belts, is presented.

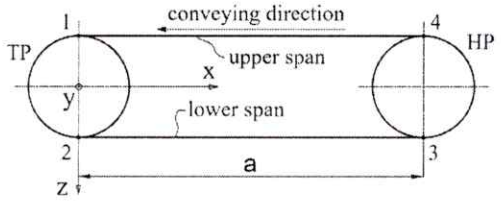

Figure 3. Nomenclature of run-up and run-off points

4.1 Highly tensioned belt: the rope model

Due to the missing bending stiffness and under the assumption of perfect static friction [2], the run-up and run-off points of both spans are connected in a straight line. As long as the pulleys are aligned parallel, the rope on the pulleys runs at a constant y-position. If, however, the tail pulley TP is yawed by the angle β, the rope begins to move sideways. A closer look at a run-up point (Figure 4) reveals the direction of the movement. From this, the chronological sequence of the lateral running (Figure 5, I - VI) and the interactions between the run-up and run-off points can be shown. The corresponding diagram with the position of these points is shown in Figure 6.

After yawing the tail pulley by the angle β (Figure 5, I), the direction of the rope deviates from the normal of the tail pulley (Figure 4). The angle difference between the direction of the rope and the normal direction of the pulley, the contact angle β_0, corresponds to the yaw angle β. When the head pulley is driven and the rope moves by the distance Δx, the point 1_0 runs sideways by the distance Δy_1 to its new position 1_1.

$$\Delta y_1 = \Delta x * \beta_0 \quad (4)$$

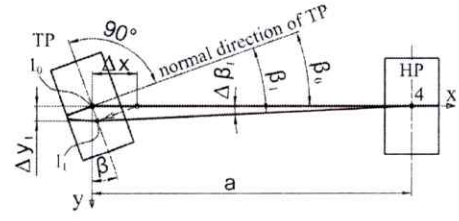

Figue 4. Geometric situation at the run-up point

The direction of the upper rope span is determined by connecting the new run-up point 1_1 in a straight line with the unchanged run-off point 4 (Figure 5, II). This reduces the contact angle by Δβ1 (Figure 4). The new contact angle β_1 can be calculated.

$$\beta_1 = \beta_0 - \Delta\beta_1 \quad (5)$$

$$\Delta\beta_1 = \frac{\Delta y_1}{a} \quad (6)$$

After half a revolution of the pulleys (Figure 5, III) the run-off point 2 begins to move sideways. The y-position of the run-off point 2 is the same as the y-position of the run-up point 1 a half pulley revolution earlier.

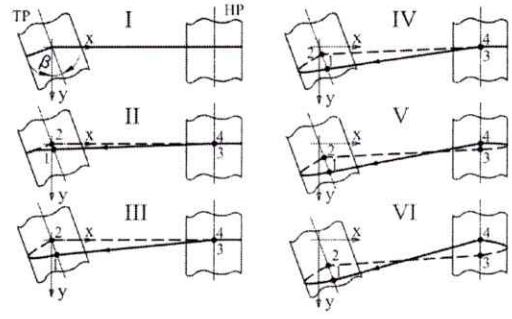

Figure 5: lateral movement of the rope

At the next step (IV) the lower rope span also begins to deflect, and the situation at the point of contact 3 of the head pulley HP begins to change gradually. As the deflection of the lower rope span increases, the contact angle at the run-up point 3 increases and the lateral travel speed of this point increases (V).

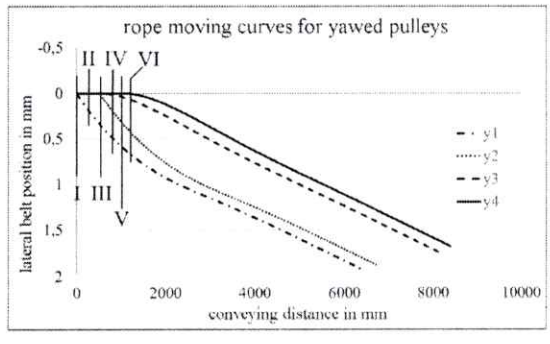

Figure 6: moving curves of a limp rope on yawed pulleys

A full pulley revolution after starting to revolute, the run-off point 4 begins to move (VI). From this time on, all four points (1 - 4) move sideways and affect each other.

The duration of the resulting stabilization process (Figure 6) depends on the geometry of the belt conveyor machine. With the dimensions of the test rig (centre distance a = 2 m, pulley radius R = 170 mm and yaw angle β = -0.042°), the oscillation decays after a few pulley revolutions and all four points move sideways at the same speed. Finally, the rope always runs sideways in the direction of the lower belt tension [2] (Figure 7).

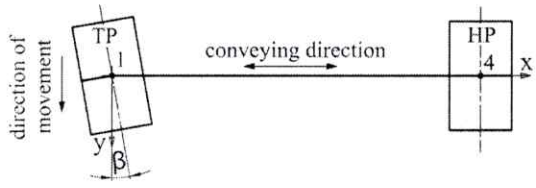

Figure 7: direction of the rope movement

4.2 Highly tensioned belt: the beam model

The lateral moving behaviour of a highly tensioned steel processing belt is also based on the geometric effects mentioned above. However, the additional bending stiffness of the belt changes the geometric conditions at the run-up point. A linear connection of the run-off point with the run-up point, as assumed in the rope model, is no longer realistic. The beam model, a mathematical model for a highly tensioned belt span consisting of a simple bending beam on two supports, is able to take this effect into account. Its bending line is used to calculate the lateral running behaviour. Due to the high tension, it is assumed that the deformation of the belt span takes place only in the belt plane and no buckling occurs. The validity of this assumption was confirmed for highly tensioned belts by measurements on a test stand [1]. With the following boundary conditions at the run-up and run-off points (7) of a belt located centrally on the pulleys and the tail pulley yawed by β

$$y(0) = 0 \quad y(a) = 0 \quad y'(0) = \beta \quad y'(a) = 0 \tag{7}$$

the equation of the bending line can be written for each belt span.

$$y'' = \frac{-M}{E * I} - \frac{\chi * q}{G * A} \tag{8}$$

For the calculation of the bending moment in the belt span, 1st order theory (Th 1. O) as well as 2nd order theory (Th 2. O) can be used [1]. The bending moment M in the belt span is calculated according to Th 1. O and Th 2. O:

$$M = M_{Th\,1.O} = -M1 - Q1 * x \tag{9}$$

$$M = M_{Th\,2.O} = -M1 - Q1 * x - F_v * (y(x) - y1_0) \tag{10}$$

If Th 1. O is applied, the equilibrium conditions on the undeformed beam are considered. When working according to Th 2. O, the deformed beam (Figure 8) is used. This makes it possible to include the preload force F_v in the equation for the bending moment. The calculation of the lateral belt position is basically done in the same way as for the rope model. In addition, the belt shape has to be considered according to the bending line. The difference between the gradient of the bending line in the run-up point and the normal direction of the pulley represents the angle of contact at this point. For the next step a new contact angel has to be calculated using the curvature of the bending line. The following process considerations for the upper belt span explain this statement in detail.

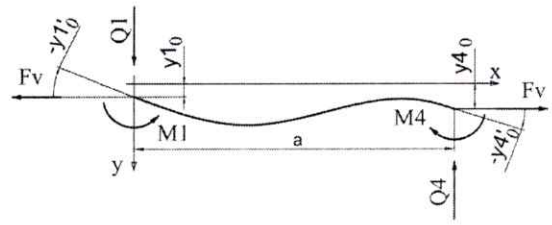

Figure 8: the beam model

Starting with the central arrangement of the undeformed belt span on the pulleys and a yaw angle β, the following situation arises for the run-up point 1_0 at timestep 0.

$$y1_0 = 0 \quad y1'_0 = 0 \quad y1''_0 \neq 0 \tag{11}$$

$$y4_0 = 0 \quad y4'_0 = 0 \quad y''4_0 \neq 0 \tag{12}$$

Since perfect static friction is assumed, the contact angle $y1_0'$ at timestep 0 equals zero. After a belt feed by Δx, the run-up point remains on its y-position.

$$y1_1 = y1_0 + y1'_0 * \Delta x = 0 \tag{13}$$

Due to the curvature $y1''_0$ of the belt span at the run-up point 1 at the timstep 0 and to the belt feed by Δx, the contact angle $y1'_1$ for the timstep 1 is different from zero.

$$y1_1' = y1_0' + y1''_0 * \Delta x \tag{14}$$

Only in the second time step the lateral movement of the run-up point 1 starts.

$$y1_2 = y1_1 + y1'_1 * \Delta x \tag{15}$$

In that way, the lateral belt movement of the belt span can be calculated for the first half pulley revolution. Then the run-off point 4 begins to move in y-direction. The boundering conditions of the beam at the run-off point will change continuously furthermore. In the next step after the mentioned half revolution, the belt leaves the pulley at point 2 at the y-position $y1_1$with the contact angle $-y1'_1$ and deflects the lower belt span. The same situation happens at point 4, with the past conditions of point 3. With these considerations, the lateral movement of the belt can be calculated analytically.

4.3 Comparison of models

To compare the models to each other, the y-position of the run-up point 1 of a steel process belt (b = 200 mm, h = 0.3 mm) with the geometry data of the test rig (centre distance a = 11.28 m, pulley radius

R = 170 mm and twist angle β = -0.042°) (Figure 11) can be calculated and visualized in a diagram (Figure 9). It can be seen that the curves of the rope model as well as those of the beam model according to Th 1. O delimit an area in which all the curves of the beam model according to Th 2. O are located. At low belt tensions the Th 2. O model behaves like the beam model according to Th 1. O. If the belt tensions are assumed to be very high, it behaves like the rope model. Consequently, the approach according to Th 2. O includes the information of the rope model and the Th 1. O beam model.

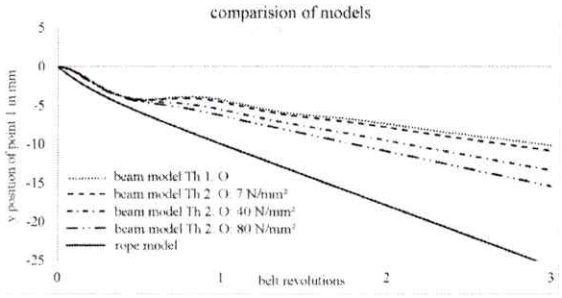

Figure 9: comparision of models

4.4 Low-tensioned belts

In order to be able to describe the effect of the decreasing tension force on the lateral running behaviour of the steel processing belt, Ritzinger [3] made fundamental considerations. The belt span is reduced theoretically to the two belt edges, wicht are defined as two independent ropes. Each of the ropes is loaded with half the weight of the belt span in the form of a rectangular distributed load. When the pulley gets yawed by β, the distances between the run-up and run-off points of the two ropes differ. This results in different sag. These saggings as well as the tension forces F_1, F_2 in the two ropes are calculated over the catenary curve. From the two tension forces and the width b of the belt a torque T_{requ} is calculated, which is required to yaw the pulley.

$$T_{requ} = (F_1 - F_2) * \frac{b}{2} \tag{16}$$

A highly tensioned belt span (width b, thickness h, length a) counteracts the yawing of the pulley by β with the torque T_{belt}.

$$T_{belt} = -\frac{4 * E * I * \beta}{a} = -\frac{4 * E}{a} * \frac{b^3 * h}{12} * \beta \tag{17}$$

Using the quotient of these two torques, the steady-state running velocity $\dot{y}_{ext}$ of a low-tensioned belt is calculated [3].

$$\dot{y}_{ext} = \dot{y}_{Th\,1.O} * \frac{T_{requ}}{T_{belt}} \tag{18}$$

These considerations according to Ritzinger provide similar results for the steady-state velocity at medium belt tensions as the beam model according to Th 2. O. If the belt tension continues to decrease, a significantly lower lateral moving speed is obtained from (18).

A new approach is to extend the existing model by considering the real position of the run-up and run-off points instead of the highest pulley position (Figure 10). With increasing the sag, the four points 1-4 move further and further away from the original position and the influence of the yaw angle β decreases. On the other hand, the influence of the roll angle from the rope's point of view increases more and more. In order to be able to include these considerations in a belt model, a suitable analytical description of the free belt spans must be found.

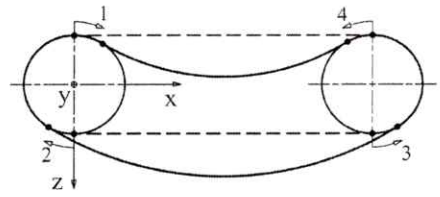

Figure 10: real position of points 1 – 4 at low belt tension

5. BEAM MODEL VS. MEASUREMENT

Before the development of further mathematical models for low-tensioned belts can be started, the behaviour of the system must be studied. The first step is to identify how the steel belt (b = 200 mm, h = 0.3 mm) actually behaves on the test rig (Figure 11: centre distance a = 11.28 m, pulley radius R = 170 mm and yaw angle β = -0.042°) when the tension is reduced.

Figure 11: test rig: center distance a = 12 m

According to the beam model Th 2. O (Figure 9), the velocity of lateral movement of the run-up point decreases with lower belt tension. This behaviour could only be partially confirmed by the measurements on the test rig. At a belt tension of 40 N/mm², the measured behaviour differs significantly from the calculated belt moving curve, but both show the same behaviour (Figure 12). If the belt tension is decreased further, two unexpected changes occur. First, the belt responds more and more slowly after yawing the pulley. The curves start less inclined (Figure 12, curve 7 and 10 N/mm²). If, however, the lateral movement has started, its speed increases unexpectedly strongly. Compared to the highly tensioned belt, the steady-state velocity of the low-tensioned belt is a lot higher.

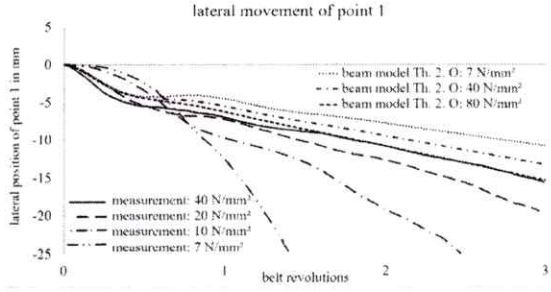

Figure 12: comparision of models and measurement

Figure 13 shows the measured values of the steady-state velocities as well as those calculated using models according to Th 1. O and Th 2. O as a function of the belt tension for the above mentioned belt with a yaw angle of $\beta = -0.042°$ for the run-up point 1.

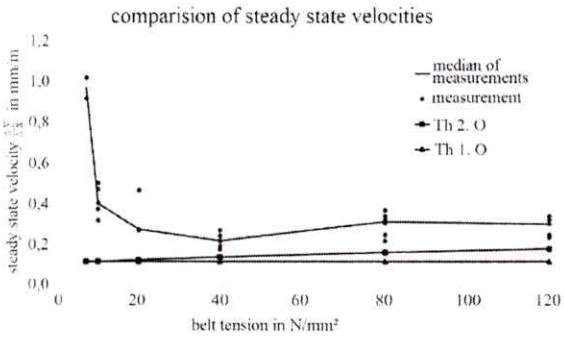

Figure 13: comparison of steady-state velocities

At a belt tension in the range of 20 to 40 N/mm², the Th 2.O model still provides quite realistic results for the steady-state velocity. If the belt tension decreases further, the characteristics of the belt will change significantly, so that the simplification of the belt deformation in one plane loses its validity. At belt tensions below 20 N/mm², its catenary is clearly visible. In addition to the known sideways deflection of the belt, yawing the pulley also results in a tilt in the cross-section of the belt (Figure 14).

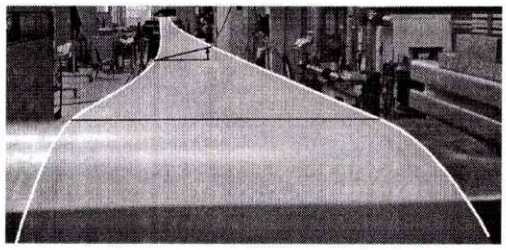

Figure 14: low tensioned belt on test rig at 10N/mm², extrem belt deformation after yawing the pulley

6. SIMULATION

In addition to analytical modelling and measurements on the test rig, the simulation of the belt movement is another method for determining the lateral running behaviour of a steel processing belt. In addition to the already mentioned parameters such as belt tension and yaw angle, the geometry of the belt machine and the belt itself can also be changed.

6.1 Finite Element Method

Koller [4] introduced an Abaqus FEM model for highly tensioned belts. He used a flat strip, meshed with S4R shell elements and rolled it into a ring so that its ends could be joined together. The pulleys were inserted into the belt ring, driven and slowly moved apart so that the belt was stretched into the correct shape. With this FEM model, the behaviour of strongly tensioned process belts was correctly visualized. Therefore these considerations as well as the procedure are continued. The aim is to be able to also describe low tensioned belts using FEM.

Otto [5] also used the finite element method to describe belt misalignment in belt conveyors. He primarily investigated the effects of geometric errors in the arrangement of the idler stations on the lateral movement of the belt.

6.2 Discrete Element Method

A new kind of simulation arises from the atypical use of the discrete element method (DEM) with the software LIGGGHTS. While DEM is typically used to describe the behaviour of bulk materials, here the belt itself is modelled from particles and placed over the pulleys of the belt machine. Since the connections between the particles can also transmit tension forces, this approach is possible. One of the aims of the DEM simulation is to create a model that can be calculated much faster than the FEM in order to predict the lateral running behaviour of a lightly tensioned belt.

ROPES:

Basic tests with high and low tensioned particle chains on two cylindrical pulleys provide the known behaviour for the rope. Figure 15 shows the movement of a highly tensioned rope and a yawed pulley at three different points in time.

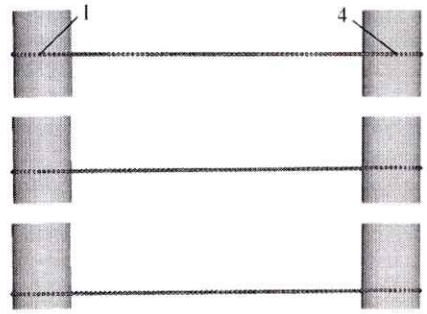

Figure 15:lateral movement of a particle chain

The corresponding diagram for the upper belt span with the run-up point 1 and the run-off point 4 is shown in Figure 16. The simulation shows the known effects such as transient oscillation, steady-state velocity and steady-state offset. Since the ropes have not yet been calibrated, a direct comparison with the analytical models at this point is not yet effective.

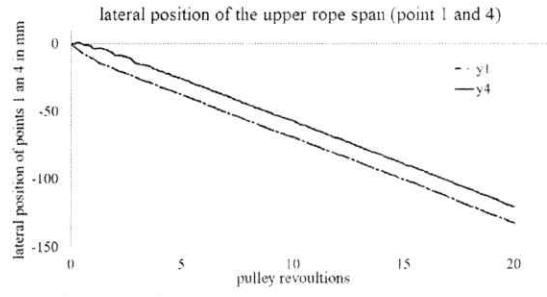

Figure 16: moving diagram for upper rope span

By increasing the rope length, low-tensioned particle chains are created. Figure 17 shows two of these chains,

each after 20 pulley revolutions. It can be seen that the position after the run is approximately the same.

Figure 17: high and low tensioned particle chains on two pulleys, shown simultaneously

BELTS:

If two or more particle chains are arranged next to each other and linked by bonds, a particle belt is formed. It can be placed on the pulleys under high tension (Figure 18) or low tension (Figure 20, above).

Figure 18: high tensioned particle belt

The simplest way to create the belt is to join the particles together longitudinally and transversely. This makes the connection of the particle chains very weak with respect to shear stresses (Figure 19). If the particles are additionally joined diagonally, the shear strength of the belt is significantly increased.

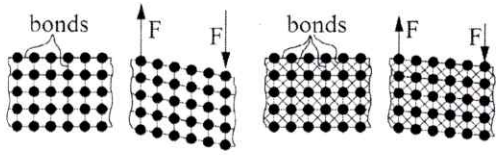

Figure 19: different types of bond arrangement

Based on these considerations, high tensioned as well as low tensioned belts can be operated on two pulleys. (Figure 20).

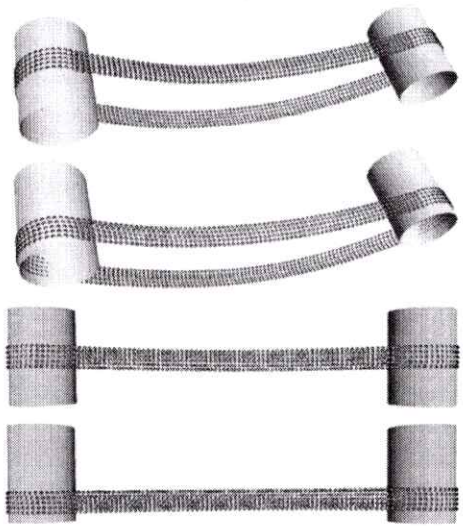

Abbildung 20: low tensioned particle belt

The corresponding belt moving diagram shows the expected behavior. Since the belt models were not yet calibrated at the time this article was written, a comparison with the analytical models or the measurement at this point is not yet meaningful. Consequently, no reliable statement can be made about the behaviour of the belt when the belt tension changes.

7. SUMMARY AND OUTLOOK

The lateral movement behaviour of a highly tensioned steel processing belt can be calculated with the beam model according to 2nd order theory. Measurements have shown that this model loses its validity with decreasing the belt tension. In order to be able to make reliable statements for low-tensioned belts, new models have to be developed. By the positions of the run-up and run-off points and with an analytical description of the belt geometry between these points, the lateral running behaviour at lower belt tension should be calculated according to the known geometric effects.

To estimate the range of validity of the known beam model with respect to belt tension, further measurements on the test rig with belts of different geometries would be desirable. In addition, the measurement results should be used to validate a mathematical model for the low-tensioned belt. In a further step, the considerations made by Koller [4] during the creation of the FEM simulation are taken up again and applied to belts with lower tension. Also the simulation with DEM seems to be helpful for the description of the lateral running behaviour of the steel belt. The work on the described models will be continued. The calibration of these DEM models is in progress.

REFERENCES

[1] Egger, M.: *Seitliches Laufverhalten des Fördergurtes beim Gurtbandförderer*, TU Wien, PHD Thesis, 2000

[2] Gabmayer, T.: *Untersuchung der Effektivität verschiedener Steuereinrichtungen zur Beeinflussung des seitlichen Laufverhaltens von Edelstahlprozessbändern,* TU Wien, PHD Thesis, 2011.

[3] Ritzinger, P.: *Seitliches Bandlauf-verhalten von langsam laufenden Metallbändern auf zylindrischen Trommeln*, TU Wien, PHD Thesis 1997

[4] Koller, M.: *Simulation des seitlichen Verlaufens von endlosen Stahl-bändern,* TU Wien, Master Thesis 2009

[5] Otto, H. and Katterfeld, A.: Prediction and Simulation of Mistracking of Conveyor Belt, The 8th International Conference for Conveying and Handling of Particulate Solids, Tel-Aviv, Vol. 8, 2015.